Published in final edited form as:
Biomaterials. 2010 July ; 31(21): 5552–5563. doi:10.1016/j.biomaterials.2010.03.051.

The Effects of Intraspinal Microstimulation on Spinal Cord Tissue in the Rat

Jeremy A. Bamford[1], **Kathryn G. Todd**[1,2], and **Vivian K. Mushahwar**[1,3,*]

[1]Centre for Neuroscience, Faculty of Medicine & Dentistry, University of Alberta, Edmonton, Alberta, T6G 2E1, Canada

[2]Department of Psychiatry, University of Alberta, Edmonton, Alberta, T6G 2E1, Canada

[3]Department of Cell Biology, Faculty of Medicine and Dentistry, University of Alberta, Edmonton, Alberta, T6G 2E1, Canada

Abstract

Intraspinal microstimulation (ISMS) involves the implantation of microwires into the spinal cord below the level of an injury to excite neural networks involved in the control of locomotion in the lower limbs. The goal of this study was to examine the potential spinal cord damage that might occur with chronic ISMS. We employed functional measures of force recruitment and immunohistochemical processing of serial spinal cord sections to evaluate any damage induced by spinal transection, implantation of ISMS arrays, and electrical stimulation of 4 hours/day for 30 days. Functional measurements showed no change in force recruitment following transection and chronic ISMS, indicating no changes to underlying neural networks. The implantation of sham intraspinal microwires produced a spatially-limited increase in the density of microglia/macrophages and $GFAP^+$ astrocytes adjacent to the microwire tracks, indicating a persistent immune response. Most importantly, these results were not different from those around microwires that were chronically pulsed with charge levels up to 48 nC/phase. Likewise, measurements of neuronal density indicated no decrease in neuronal cell bodies in the ventral grey matter surrounding ISMS microwires (243.6/mm^2 ± 35.3/mm^2) compared to tissue surrounding sham microwires (207.8/mm^2 ± 38.8/mm^2). We conclude that the implantation of intraspinal microwires and chronic application of ISMS are well tolerated by spinal cord tissue.

Introduction

Spinal cord injury represents a devastating neurological impairment with potentially life-threatening implications. Following injury, a host of challenges to quality of life arise and typically involve impaired bladder and bowel function, respiration, skin and muscle health, freedom of movement, and general independence. Previous interventions have applied

*Corresponding Author: Dr. Vivian Mushahwar, Department of Cell Biology and Centre for Neuroscience, 5005 Katz Group-Rexall Centre for Pharmacy and Health Research, University of Alberta, Edmonton, Alberta, T6G 2E1, Canada, (780) 492-4519 (phone), (780) 492-1617 (fax), vivian.mushahwar@ualberta.ca.
Co-authors: Jeremy A. Bamford, Centre for Neuroscience, 5005 Katz Group-Rexall Centre for Pharmacy and Health Research, University of Alberta, Edmonton, Alberta, T6G 2E1, Canada, Kathryn G. Todd, Department of Psychiatry and Centre for Neuroscience, 5005 Katz Group-Rexall Centre for Pharmacy and Health Research, University of Alberta, Edmonton, Alberta, T6G 2E1, Canada

functional electrical stimulation (FES) to address these problems with some success (For reviews see [1-3]).

Intraspinal microstimulation (ISMS) is an FES approach that targets the lumbosacral enlargement, a small region in the spinal cord that controls the movements of the legs. We demonstrated that stimulation in this region produces coordinated whole-leg movements. Patterned ISMS through as few as four microwires in each side of the spinal cord is capable of producing prolonged weight-bearing standing [4] and stepping [5] in adult cats. A hallmark of ISMS is its gradual recruitment of force which is due to its orderly, preferential recruitment of small, fatigue-resistant motor units [6]. This characteristic is attributed to the trans-synaptic activation of motoneurons through a larger network of afferent projections, interneurons and propriospinal neurons activated by ISMS [3,7], and partially explains the prominent fatigue-resistance produced by ISMS in movements such as standing and stepping compared to other FES approaches [4,5]. Collectively, the findings from ISMS to date suggest that it may be a viable method for restoring standing and walking capacity after spinal cord injury.

Nonetheless, the insertion of intraspinal microwires and subsequent electrical stimulation could potentially cause damage within the spinal cord. The mere implantation of foreign bodies into central neural tissue is associated with initial traumatic injury and an ongoing inflammatory response [8]. In implants related to peripheral nerve stimulation, previous authors have shown that much of the damage arises from the mechanical strain imposed by the implant upon the nerve [9]. Central stimulation paradigms have the advantage of anchoring neural prostheses to hard, bony structures and implanting microelectrodes within relatively immobile neural tissues; however, mechanically mismatched or unstable implants could cause severe damage to the surrounding tissue.

In addition to mechanical damage, the ongoing electrical stimulation may cause trauma due to the injection of charge. This can occur due to potential cytotoxic effects at the electrode-tissue interface [10] or due to the flow of current across the neural structures [11]. In addition, the duty cycle of electrical stimulation can damage the excited neurons if the interaction between stimulus frequency and daily stimulus duration reaches harmful levels [12]. Thus, even if the discrete pulse parameters are not injurious, the aggregate chronic stimulation protocol may become so if the neural structures are excited at too high a rate or for too long.

The purpose of the current work was to evaluate the response of the rat spinal cord to microwire implantation and 30 days of ISMS. Immunohistochemical procedures were used to reveal any damage induced by the insertion of microwires and subsequent stimulation. This was examined directly at the spinal cord level and functionally by evaluating the recruitment of force following microwire implantation and 30 days of ISMS. The experimental protocol involved stimulation through two microwires on one side of the spinal cord. On the contralateral side, two microwires were implanted as sham controls and were not used for stimulation. Stimulation proceeded daily for 4 hours with a 50% duty cycle of one second on and one second off. This protocol was chosen to approximate the anticipated duration of daily use of the ISMS system upon clinical translation. The degree to which this protocol could induce damage and/or alterations in the pattern of recruitment of motoneurons was assessed.

Materials and Methods

Animals

Experiments were performed on a total of 13 Sprague-Dawley rats weighing 225-275 g. All procedures were approved by the University of Alberta Animal Welfare Committee and were in keeping with the guidelines for scientific research in animals approved by the Canadian Council on Animal Care.

Spinal cord transection

Aseptic transection of the spinal cord at the eighth thoracic vertebra (T8) was carried out as follows. Under 2.0 % isofluorane anesthesia, a laminectomy was performed to expose the T8 spinal segment. The spinal cord was cut progressively from the dorsal to ventral aspects and the lesion site was closely inspected to ensure that no tracts remained intact. Surgical mesh was inserted into the cavity to minimize bleeding and a thin layer of plastic film was glued in place over the laminectomy site to prevent the invasion of connective tissues. The wound was sutured closed and analgesics (buprenorphine 0.015 mg/kg sc) and antibiotics (enroflaxacin 1.0 mg/kg sc) were administered. Analgesics were subsequently administered as needed along with a one week course of daily antibiotics. The animals' bladders were expressed manually 3 times per day for two weeks, and once daily thereafter. Animals were singly housed and cages were inspected daily and changed at least twice per week. A total of 10 animals were transected in this manner. In order to account for the effects of spinal cord transection alone, 4 of these 10 animals received only the transection and were classified as spinal cord transected control (ST).

ISMS Implant

After a two week recovery period, a second laminectomy was performed on 6 transected animals to expose spinal cord segments T13 and L1. ISMS microwire arrays were implanted as described previously in rats [6,13] (Figure 1). Arrays of 4 wires, 1.5 mm in depth, were manufactured from 30 μm-diameter platinum-iridium microwire (California Fine Wire, Grover Beach, CA, USA) according to established protocols [14]. The wires were insulated with 4 μm polyimide except for the tip. After sterilization, the arrays were inserted with two microwires in each side of the spinal cord and a 2 mm-spacing between rostral and caudal wires. The target location of the microwire tips was the quadriceps motoneuron pool in the ventral grey matter of the spinal cord, which was previously mapped [15].

Microwires were fixed to the dura mater with individual drops of cyanoacrylate glue at their point of insertion. They were then routed upon the dorsal surface of the dura mater to the base of the T12 vertebrae, where they were collectively sutured to the dura mater using 8-0 silk (Figure 1). A thin layer of plastic film was glued over the implantation site to prevent the adherence of overlaying muscle to the implanted array. At the T12 spinous process, microwires were routed through a silastic tube to a headpiece (MS363, PlasticsOne, Roanoke, VA, USA) which was fixed to the rat skull using stainless steel screws and dental acrylic. Muscle and skin layers were sutured and analgesics were administered (buprenorphine 0.015 mg/kg sc). All animals were given a one week recovery period during which they received daily bladder expression and no ISMS.

Stimulation protocol

One side of the spinal cord was selected for daily stimulation and was designated ISMS, while the contralateral side was chosen as the unstimulated sham control and was designated intraspinal microwire control (ISC). The ISMS side was stimulated for 4 consecutive hours of every day for 30 days through the two ipsilateral microwires, while the contralateral ISC side received no stimulation. Individual ISMS pulses were 200 μs in duration, biphasic, charge balanced, cathodic-first. Stimulus trains of 25 pulses per second (pps) were delivered through each microwire in an interleaved manner to produce 50 pps contractions in the quadriceps muscle. Interleaved stimulation presents interposed stimulus pulses from multiple electrodes at evenly spaced intervals [10].

Stimulation proceeded for one second followed by one second of rest and was carried out at a level sufficient to produce functional contractions of the quadriceps muscle. Stimulus threshold levels for the activation of the quadriceps muscle were measured approximately every 10 days

and, when necessary, stimulus amplitudes were adjusted to maintain similar levels of functional contractions. Stimulus amplitudes were maintained between 140 - 260 μA, or 28 - 52 nC per phase. This represented a mean of 2.55 ± 0.87 times the stimulus threshold level for quadriceps muscle activation. Stimulating at these levels produced functional contractions from the ipsilateral quadriceps muscle in each animal throughout the 30 day stimulation period.

Functional assessments in terminal experiments

Muscle force recruitment curves were obtained from 3 of the 6 animals that underwent chronic ISMS and were compared to curves obtained from 3 intact animals. Under isofluorane anesthesia, animals were positioned in a stereotaxic setup which held the experimental hind limb rigidly in space. The patellar ligament was dissected free from its point of insertion on the tibia, and sutured to a force transducer (Interface MB-5, Interface Inc., Scottsdale, AZ, USA). The existing microwires where used for ISMS in the spinal and chronically implanted rats while pairs of ISMS microwires were implanted on the day of the experiment in the intact rats. The microwire tips targeted the quadriceps motoneuron pool as with the chronic implants. Isometric force recruitment curves were generated by stimulating through each microwire individually at 25 pps. A second set of force recruitment curves were generated by stimulating through both microwires simultaneously with the 25 pulses interleaved to produce an aggregate 50 pps activation frequency. Stimulation amplitude was varied randomly from sub-threshold to a maximal amplitude of 400 μA, and the evoked forces were recorded. Using the same protocols, force recruitment curves were generated using 5 microwires in 3 animals that had been stimulated for 30 days through the chronically implanted wires, and 6 ISMS microwires in 3 intact animals with acute implants.

Perfusion and Tissue Handling

One day after the final day of chronic ISMS (i.e., the 31st day) animals were euthanized, perfused through the heart and the spinal cords were removed. The perfusion proceeded with the delivery of approximately 200 ml of saline at a rate of 40 ml/min, followed by 200 ml of 4% formalin solution at the same rate. The implant site was exposed and the microwires were removed. The spinal cords were then excised and soaked in formalin solution overnight. Subsequently, cords were transferred to 20% sucrose/phosphate buffered saline (PBS) at pH 7.4 for cryoprotection. Cryoprotectant solution was changed daily for 7 days until all cords sank to the bottom of the solution. Cords were embedded in cryostat tissue mounting medium and frozen by submersion in isopentane cooled in liquid nitrogen. Cords were subsequently stored at -80° C until serial cross sections of 20 μm thickness were cut using a cryostat and thaw mounted onto slides (Superfrost plus gold, Fisher Scientific, PA, USA).

Immunohistochemistry

To evaluate the potential tissue damage induced by microwire implantation and ISMS for 30 days, immunohistochemistry using antibodies recognizing various relevant antigens was performed. Serial sections were immunoreacted with antibodies recognizing the neuronal marker NeuN (clone A60) to determine the density of neurons in the region of the implant, microtubule associated protein-2 (Map-2, clone HM-2) to evaluate cytoskeletal disruption, glial fibrillary acidic protein (GFAP, clone GA5) to identify reactive astrocytes, and ED-1 (clone ED-1) to identify macrophages and microglia. To assess synaptic terminals, antibodies recognizing synaptophysin (polyclonal) were used.

Serial sections at 200 μm intervals along the spinal cord segments where microwires were implanted were used for each immunoreaction. As such, the separation between serial tissue sections immunoreacted with a given antibody was 200 μm in either the rostral or caudal direction. To ensure optimal antigen recognition, a standard antigen retrieval technique was applied [16]. Slides with mounted tissue cross-sections were incubated at 95 °C for 20 min in

10 mM citrate buffer at pH 6.0. Slides in buffer were then removed from the heat and left to cool at room temperature for 20 min until the buffer reached an approximate temperature of 50 °C. Slides were then rinsed in distilled water and a standard immunohistochemical staining procedure was followed. Briefly, slides were incubated for one hour at room temperature in blocking solution containing PBS-tween, 1% bovine serum albumin, 10% horse serum and avidin-D blocking agent (Vector Laboratories, Burlingame, CA, USA). The blocking step for synaptophysin was identical except for the substitution of goat serum for an equal amount of horse serum. Incubation with the primary antibodies was overnight at 4 °C (NeuN 1:2000; Map-2 1:2000; ED-1 1:800; GFAP 1:400; synaptophysin 1:800) in blocking solution which also included biotin blocking agent (Vector Laboratories). Sections were then incubated with the appropriate secondary antibodies (1:400) for one hour at room temperature. Subsequently, sections were incubated for one hour at room temperature with Vectastain ABC Reagent (Vector Laboratories) in PBS and immunoreactivity was visualized using the chromagen diaminobenzidine with NiCl. To halt the developing reaction, sections were rinsed with distilled water and dehydrated in solutions of increasing ethanol concentration before clearing in xylene and mounting with Entallan mounting medium.

Imaging and Post-Processing

Digital photomicrographs of immunoreacted serial sections were obtained using a Leica DMLS microscope (Leica Microsystems, Wetzlar, Germany) and attached digital camera (Spot Insight, Diagnostic Instruments, Sterling Heights, MI, USA). Representative images selected for publication were post-processed using commercial imaging software (Photoshop CS4, Adobe Systems Incorporated, San Jose, CA, USA). Standard post-processing methods were applied to these images including the adjustment of brightness and contrast according to approved methods [17].

Neuronal density was measured by counting the number of NeuN-positive ($NeuN^+$) cells in the vicinity of implanted microwire tips in the ventral horns of both ISMS and ISC sides of the chronically implanted animals, and in matched areas in the ST control group. The number of positive cells in laminae VII-IX was divided by the area analyzed to give a measurement of neuronal density in ISMS, ISC and ST control groups, expressed as cells/mm^2. The investigator responsible for counting $NeuN^+$ cells was blinded to treatment groups.

Statistics

All analyses were performed with a computerized software package (SPSS 17.0, SPSS Inc., Chicago, IL, USA). Differences between groups were determined using one-way ANOVA and Tukey HSD post hoc analyses. Paired t-tests were performed between results from the ISMS side and the contralateral unstimulated ISC side where appropriate. All data are presented as mean ± standard deviation. Differences were considered significant at $P < 0.05$.

Results

Microwire tip locations

The locations of implanted pulsed and unpulsed intraspinal microwire tips were verified directly in spinal cord cross-sectional slices. The locations of ISMS microwire tips are shown in Figure 2. Of 24 microwires implanted in 6 animals, a total of 16 were located on stained tissues. Presumably, some sections showing the microwire tips were lost during tissue processing including sectioning on the cryostat and immunohistochemical staining. Since the diameter of implanted microwires is only 30 μm, it is possible that the loss of a few 20 μm thick tissue sections in certain areas would make the localization of all microwire tips rather difficult. As shown in Figure 2, all of the located microwire tips were in the ventral grey horn.

Intraspinal microwire stimulus thresholds

The stimulus threshold amplitudes for quadriceps muscle activation were tested on the first day of ISMS and approximately every ten days thereafter (Figure 3). Mean threshold for muscle activation with ISMS microwires dropped significantly from 118.2 μA ± 45.1 μA to 67.8 μA ± 25.1 μA by the end of the 30 days of stimulation. This represented a mean decrease in threshold of 33.6% ± 38.2%. The mean slope of regression curves fitting stimulus threshold vs. time was -1.61 ± 1.67, indicating the decline in stimulus threshold during the 30 day period. One microwire (out of 12) failed permanently on the 14th day of stimulation while the remaining 11 lasted throughout the 30 day stimulation period. Stimulus thresholds decreased in 8 of the microwires, increased in two, and showed no overall change in one.

Recruitment properties of ISMS

The slopes of the regression lines between stimulus amplitude and normalized force in intact animals were 0.0034 ($R^2 = 0.68$) and 0.0038 ($R^2 = 0.79$) for individual microwires pulsed at 25 pps and two microwires pulsed in an interleaved fashion at 50 pps, respectively (Figure 4 A,B). Following chronic ISMS, the slope of the regression line between stimulus amplitude and normalized force with microwires pulsed at 25 pps was 0.0034 ($R^2 = 0.78$, Figure 4C). An analysis of covariance indicated that these regression lines were not significantly different from one another. Given this, we conclude that the recruitment of force through ISMS is not altered following spinal cord transection and 30 days of daily ISMS. This suggests that ISMS continues to activate the neural circuitry of the spinal cord of chronically stimulated animals in the same manner as in the acute animals. This also suggests that chronic ISMS does not cause sufficient tissue damage to compromise the underlying neural networks that produce graded force recruitment.

Inflammation and reactive gliosis

Microwires were affixed to the T12 spinous process and run along the dorsal surface of the dura mater. In two cases, microwires invaginated into the dorsal funiculi of the spinal cord (Figure 5). This caused some deformation of the grey matter and recruitment of monocytes to surround the embedded microwires (Figure 5C). Encapsulation of the microwires and an increase in GFAP immunoreactivity were noted (Figure 5D). In these instances, damage to the dorsal grey matter did not appear to be severe as there were numerous $NeuN^+$ cells in the dorsal horn after 30 days of implantation, suggesting that dorsal neurons were not killed by the deformation of the dorsal horn and surrounding white matter (Figure 5B). In addition, Map-2 immunoreactivity, a marker of the neuronal cytoskeleton [18,19], was present and was not apparently diminished on the stimulated side as compared to the unstimulated side. (Figure 5A). Nevertheless, since damaged neurons may still express NeuN, it remains possible that neurons in the dorsal horn may have been compromised by the invagination of the microwires. Furthermore, the functional consequences of the observed displacement and deformation of the dorsal white and grey matters are unknown.

Microwires within the spinal cord were surrounded by large, GFAP-positive ($GFAP^+$) cells that we identified as reactive astrocytes along the length of the microwire (Figure 6). In addition, a concentration of ED-1 positive ($ED\text{-}1^+$) cells in the microwire track demonstrated the recruitment of macrophages and microglia to the damaged area (Figure 6). The extent of encapsulation, reactive astrocytosis and immune response did not appear to vary along the length of the microwire track or at the microwire tip. ED-1 immunoreactivity proved to be the best way to identify microwire tracks as we observed an elevation in ED-1 labelling in all microwire tracks of adjacent serial spinal cord tissue sections, 200 μm in the rostral or caudal directions. However, the ED-1 response had faded by the next cross section, a total of 400 μm distance from the microwire track. In some spinal cord sections we noted pieces of insulation along the microwire tracks of both pulsed and unpulsed microwires and, in some

instances, at the dorsal cord surface at the site of microwire penetration (Figure 5B, 6H and 7E). We believe portions of the insulation were stripped from the microwires during explantation instead of breaking off at some point during the 30 day stimulation period because they were free of encapsulating tissues and often rested on top of the spinal cord section.

Neuronal density

Analyses of NeuN immunoreactivity showed a similar density of neurons throughout the grey matter in spinal tissue from ISMS, ISC and ST unimplanted animals (Figure 7). Presumably, the insertion of microwires caused the death of neurons directly in the path of insertion and the displacement of others adjacent to the shaft of the implanted microwire or subjacent to the tip. Subsequent stimulation, however, did not appear to lessen the number of $NeuN^+$ cells around the tracks of pulsed microwires. Specifically, counts of $NeuN^+$ cells in the ventral grey matter showed no significant differences in mean neuronal density between ST, ISC and ISMS groups (Figure 8A). Furthermore, there was no significant correlation between the levels of increasing charge injection and neuronal density (Figure 8B). The range of neuronal densities in ventral grey matter was 180 - 264 $NeuN^+$ cells/mm^2, 190 - 287 $NeuN^+$ cells/mm^2 and 174 - 288 $NeuN^+$ cells/mm^2 in ST, pulsed ISMS and unpulsed ISC spinal cords, respectively. The nearly identical ranges between ISMS and ISC suggest that stimulation up to 48 nC/phase and 25 pps for 4 hours per day does not cause the die-off of nearby neurons.

Structural damage and synaptic reorganization

Immunoreaction with the Map-2 antibody were used to identify motoneurons and neural processes in the ventral horn (Figure 9). In the ventral grey matter large, polygonal neurons with clearly observed projections into the white matter were identified as motoneurons. The staining pattern demonstrated with the Map-2 antibody was consistent with previous reports of Map-2 immunoreactivity in the spinal cord [18,19]. We observed no apparent differences in staining pattern or intensity between ISMS, ISC and ST controls. Moreover, a survey of tissues within 200 μm of implanted microwires showed no alteration in the intensity or distribution of Map-2 immunoreactivity that would indicate damage to the cytoskeleton of neurons.

Tissues immunoreacted with the synaptophysin primary antibody displayed punctate reaction products around the edges of large, polygonal neurons in the ventral horn, presumably motoneurons, with some less intense reaction of the soma (Figure 10). The staining pattern of the synaptophysin immunoreactivity was similar to that observed previously around spinal cord motoneurons [20]. There were no apparent differences in the pattern or intensity of snyaptophysin immunoreactivity throughout the ventral horn between ISMS, ISC and ST controls. Likewise, there were no apparent qualitative changes in synaptophysin immunoreactivity in the ISMS, ISC and ST control groups within 200 μm of implanted microwires.

Discussion

Overview

Intraspinal microstimulation is a paradigm of electrical stimulation designed to reanimate paralyzed legs by exciting directly the neural circuits in the spinal cord which control the muscles below the level of a spinal lesion. This involves the chronic implantation of fine microwires into spinal tissue and subsequent stimulation at levels sufficient to excite neural tissue adequately to produce desired levels of muscle activation. Multiple microwires are needed for the coordinated activation of muscle synergies necessary for complex movements such as standing and walking [3]. In the current work, we found that the mechanical implantation of microwires resulted in their encapsulation by reactive astrocytes and

monocytes. This is typical of the foreign body response observed during implantation of electrodes into the nervous system [21]. Despite this, there was no significant decrease in neuronal density and no apparent disruption of the cytoskeletal elements in the ventral horn surrounding the implant. This is encouraging given the exaggerated mechanical mismatch between the size of the rat spinal cord and the 30 μm diameter microwires that were implanted in this study. Typically, these microwires are implanted in cats with much larger spinal cords and have demonstrated very little damage [1]. Furthermore, the damage caused by implantation was not exacerbated by subsequent stimulation for 30 days at a level sufficient to activate strongly the quadriceps muscle in rat. Although there were significant decreases in the stimulus threshold of the quadriceps muscle group, we found no apparent increase in synaptic density on motoneurons and no change in the recruitment of force by ISMS following 30 days of ISMS. We conclude that functional activation of skeletal muscle through ISMS can be achieved safely; however, more compliant implants insulated by more robust polymeric materials would further minimize the mechanical damage associated with chronic implantation.

Functional recruitment

Motor units recruited during voluntary or reflex actions follow a specified order proceeding from smallest to largest. This is known as the size-principle and is explained by the rheobase current for motoneurons as well as the organization of synaptic input to motoneurons [22]. Following spinal cord transection in cats the principle of ordered recruitment according to motor unit size can be lost and a disordered recruitment profile can be observed transiently [23,24]. Although the reasons for disrupted recruitment order are uncertain, it may be explained by an increase in the magnitude of heteronymous excitatory postsynaptic potentials (EPSPs) to extensor motoneuron pools following transection [25]. One report of this phenomenon also suggested that the increase in EPSPs is largest in fast fatiguable, and fast fatigue-resistant motoneurons shortly after transection [26]. The size of EPSP magnitudes does return to normal after several months which roughly coincides with the return of an ordered recruitment pattern. ISMS in intact animals takes advantage of the extant circuitry in the spinal cord by activating a larger network of afferent projections, interneurons and propriospinal neurons, and in turn produces a graded recruitment of force [4,6,7].

Given the possibility of disordered recruitment following spinal transection and the potential plastic alterations to spinal cord circuits caused by chronic ISMS, it was important to determine if force recruitment properties from the ISMS animals would be similar to those produced in intact animals. In the current work we showed that the slope of the relationship between normalized force and stimulus amplitude obtained from intact animals is not altered following chronic transection and 30 days of ISMS, indicating the ability of ISMS to recruit force gradually in an animal model with chronic spinal cord injury.

Ongoing inflammatory response

One finding of this study is that chronic ISMS for 30 days did not worsen the initial damage induced by the insertion of microwires into the spinal cord. Upon removal of the chronically implanted microwires the tracks were extremely difficult to detect in cross-sectional slices before staining. Immunostaining for ED-1 proved to be the best indicator of the microwire track location as it produced a strong signal in and around the microwire tracks. Elevated immunoreactivity for ED-1 was observed at 200 μm rostral and caudal to the microwire tracks but not at 400 μm. In cross-sectional slices beyond this point, no indication of implantation could be found; thus, the immune response caused by microwire insertion was limited to a distinct area surrounding the microwire implants which extended further than 200 μm but less than 400 μm in rostral and caudal directions.

The classical understanding of spinal cord damage suggests that activated monocytes are recruited within the first few days following injury and that this response subsides in the following weeks [27]. Our results showed that there was a persistent inflammatory response to the intraspinal microwires 38 days after implantation. The tracks of chronically implanted microwires were found to contain clusters of ED-1$^+$ cells indicating an ongoing inflammatory response. This may be explained by the fact that the implants in question cannot be broken down and absorbed by the immune system, thus incurring an ongoing response. Other authors found similar results with silicon electrodes implanted in rat cerebral cortex for up to 4 weeks [8]. These authors demonstrated that an acute stab wound with the microelectrode did not show macrophage/microglia recruitment 4 weeks later while the implanted electrode produced a persistent inflammatory response similar to that observed here. The existence of an inflammatory response, ongoing after 38 days, raises the issue of long-term stability and safety of implanted microwires. Activated microglia and macrophages are responsible for the release of compounds such as cytokines and tumor necrosis factor-α [28]. These factors encourage the continuing immune response and can have cytotoxic effects.

Previous authors have also shown a decrease in neuronal content surrounding implanted microelectrodes and suggested that the cause might be the cytotoxic elements released by the ongoing inflammatory response they observed [8,29]. Although similar to their findings we observed a persistently elevated ED-1 immunoreactivity, we found no decrease in neuronal density around either pulsed or unpulsed microwires. The difference may lie in the nature of the implanted electrodes. Other implanted microelectrodes have a very different footprint measuring 200 μm wide by 15 μm thick at the base, and tapering to 33 μm wide and 2 μm thick at the tip. In addition, due to their silicon construction those implants are much stiffer than the 30 μm diameter platinum-iridium microwires used in this study. It is reasonable to expect that stiffer implants might produce greater damage as more flexible electrodes are better able to yield with any movement in the surrounding tissue. Indeed, the same authors concluded that the decreased neuronal content surrounding a neural implant tethered to the skull, as opposed to a floating design, may have been due to the combination of micromotion of the implant within the tissue and the stiffness of silicon implants [29].

Previous work with deep brain stimulation (DBS) implants in humans showed no ongoing inflammatory response or tissue damage in autopsied brains from patients who had active implants for up to 70 months before their deaths [30]. This suggests that the persistent immune response observed around the implanted microwires in the present study will ultimately recede. The same work also demonstrated well preserved neurons and synaptophysin-immunoreactive bodies close to the implantation tracks, a finding similar to our own.

Reactive gliosis

In addition to the ongoing recruitment of monocytes, the microwires were bordered by a thin (< 50 μm) gliotic layer immunoreactive for GFAP (Figure 6C, D, G, H). This reactive gliosis was observed around the implanted microwires, both in the ventral horn and at the dorsal surface where the microwires were routed to a silastic tube. There was no apparent difference between the encapsulation of pulsed or unpulsed microwires. The thickening of the glial sheath in the weeks following implantation has been associated with the degradation of signal and ultimate failure of recording electrodes [21]. In the case of stimulating electrodes, the glial sheath is likely to be less of an impediment to the operation of the electrodes but could increase the amplitudes of stimulation thresholds [31]. In this particular study, stimulation thresholds were unaffected by the gliotic layer and slightly decreased over time.

Reactive gliosis around neural implants is a common finding [21] and has been shown to persist for years as evidenced by autopsies of deep brain stimulators implanted into human patients [30]. The progression of encapsulation surrounding the implant, specifically the increase in

GFAP immunoreactivity, has been associated with an increased tissue adherence to the implant and resistance to removal of chronically implanted electrodes [32]. This may explain our observation that some of the chronically implanted microwires retained some surrounding scar tissue when removed, leaving both a tissue residue on the microwire and, in two cases, an enlarged cavity in the spinal cord with no sign of connective tissue or a glial scar (Figure 7G, H). Other authors have noted similar findings with silicon microelectrodes at 2 and 4 weeks after implantation [33]. At later time periods the glial sheath becomes more compact and the adherence between tissue and electrode surface is lessened resulting in less damage to the tissue when electrodes are removed.

In concert with this finding we observed pieces of polyimide insulation at multiple locations around the microwire tracks in the tissue cross-sections. Presumably, these pieces were stripped off from the implanted microwires. The pieces were gold in color and were found within and around the microwire tracks (see Figure 5B, 6H and 7E). It is unclear when the insulation was removed but we suspect that it occurred during the withdrawal of microwires from spinal tissue and not during the 30 day stimulation period. This is so because the insulation pieces were found surrounding both pulsed and unpulsed microwires. Moreover, the deposition of these pieces was uniform along the length of the microwire track instead of being focused at the microwire tip where the stimulation occurred. Pieces of insulation appeared to be free from encapsulation by connective tissues and, when intermingled with tissues, were observed to be resting on top of the tissues.

Structural damage

Synaptic reorganization during recovery from trauma can be visualized by alterations in neuronal cytoskeleton and synaptic input via immunoreactivity for Map-2 and synaptophysin, respectively [18-20]. In normal conditions Map-2 immunoreactivity reveals neurons and dendrites [34] while synaptophysin immunoreactivity on motoneurons is punctate and discontinuous revealing synaptic inputs onto the neuron [35]. Following trauma, diminished Map-2 staining indicates structural damage to the neuron while a decrease or absence of staining for synaptophysin around the soma indicates a loss of descending, propriospinal and afferent input. We observed similar Map-2 staining of motoneurons and perineural areas from ISMS, ISC and ST controls. Likewise, we found no apparent difference between ISMS, ISC and ST controls in synaptophysin immunoreactivity surrounding motoneurons in the ventral horn. These observations align closely with previous descriptions of punctate, discontinuous synaptophysin staining patterns around undamaged neurons suggesting that any loss of synaptophysin immunoreactivity following spinal transection was restored in all groups by the time of the terminal experiments. Importantly, the chronic implantation of microwires and subsequent ISMS did not cause a loss of synaptic input to the motoneuronal somata. Our findings are similar to those obtained in tissue of human patients with chronic DBS implants where regular staining for synaptophysin in close proximity to pulsed electrode tracks was observed [30].

Plasticity

We have previously shown that chronic implants in the cat spinal cord undergo an increase in stimulus threshold within the first 10-15 days followed by long periods of stable thresholds [31]. Presumably this was due to the effect of encapsulation around the microwire tip. Given these previous results we were surprised by the current finding that stimulus thresholds decreased in the first two weeks after the initiation of stimulation and then stabilized. This may be explained by the fact that the previous work did not entail daily stimulation as the current work did. It is possible that the significant decline in stimulus threshold for quadriceps muscle activation is the result of a mechanism similar to that seen during training in chronically transected cats and rats [36]. The authors of this work showed an increase in the expression of

markers of inhibitory neurotransmitters in the transected cord which was reversed with activity in the form of physical training. A decrease in the stimulus threshold could be achieved through a similar mechanism following chronic activation of circuits by electrical stimulation.

Microwire design

The current work represents the first study to assess the chronic effects of daily ISMS. It is also the first to use a rat model to evaluate the ISMS implants chronically. The rat spinal cord is considerably smaller than that of the cat, our previous animal model. This makes accurate targeting of the microwire tips in the ventral horn more challenging and creates a mechanical mismatch between the 30 μm diameter microwires and the smaller cord diameter of the rat. Some of the damage caused by insertion of the microwires can be attenuated by addressing the materials, design and implantation techniques relevant to ISMS microwires. The invagination of microwires into the dorsal horn in two cases (Figure 5) is likely due to a downwards force upon the microwire which may have occurred during or after the implantation. During the implantation procedure it is possible that the microwire was inserted with too much force, causing it to be pushed into the tissue along with the inserted tip and shaft. However, it seems more likely that this occurred afterwards due to a downwards pressure placed upon the implant by the muscle and skin layers that were sutured closed over the implant. Given that this damage has not been observed in cat implants, it may be related to the relatively smaller space between the spinal cord and the muscle layers in the rat. Thus, this particular form of damage seems unlikely to occur in cat or human procedures. The polyimide insulation used in the current design has been shown to be relatively non-toxic and compliant [37]; however, we found that pieces of this insulation were stripped from the microwires during explantation. Although we do not believe this occurred prior to explantation, it may indicate that the robustness of the insulation material needs to be improved.

A great deal of controversy and mixed results surround the question of speed of implant insertion into the tissue, perhaps owing largely to the wide array of electrode designs currently in use (as reviewed in [37]). When inserting stiffer arrays, some authors have suggested implantation at high speed using microdrivers [38]. However, given the advantages of flexible microwires in yielding with the motion of the surrounding tissue it seems that hand implantation at relatively slow speeds remains the best option for our flexible microwire implants. Some of the microelectrodes used by others have rounded tips which can cause a compaction of neurons around the microwire tip [39]. We observed a similar phenomenon in one instance (Figure 7H); however, this was not common with our implants. This is likely due to the fact that these microwires have sharpened tips which are better able to advance through tissue than a rounded tip.

Conclusions

We found that implantation of intraspinal microwires caused limited encapsulation with reactive astrocytes and an inflammatory response which persisted until the terminal experiment. There was, however, no diminishing of neuronal density in the ventral horn near the microwire tracks, nor any sign of cytoskeletal damage. Microwires which were used for daily stimulation with charges up to 48 nC/phase and a rate of 25 pps showed no more damage than those which remained unpulsed. In comparison to spinal controls we conclude that chronic ISMS produces limited damage due to the initial insertion of microwires which is not worsened by daily stimulation at levels sufficient to cause functional activation of the quadriceps muscle group. Moreover, the force recruitment properties of ISMS were unaltered following spinal transection and 30 days of ISMS. Although chronic activation of spinal cord circuitry can reasonably be expected to encourage activity-induced plasticity, we observed no alteration in the pattern of staining with the synaptophysin antibody.

These results are very encouraging, especially given the dramatic mechanical mismatch between the relatively small rat spinal cord and the 30 μm diameter microwires, and suggest that ISMS is a safe procedure for long-term use in restoring function after spinal cord injury. Nonetheless, it would be prudent to continue the effort to limit damage during implantation. This can be accomplished by redesigning the microwires with more compliant and robust materials and by examining the techniques of implantation.

Acknowledgments

The authors would like to acknowledge Dr. Jan Kowalczewski for the artwork in Figure 1.

Sources of support: Alberta Heritage Foundation for Medical Research, Canadian Institutes of Health Research, International Spinal Research Trust, National Institutes of Health

References

1. Prochazka A, Mushahwar VK, McCreery DB. Neural prostheses. J Physiol 2001;533:99–109. [PubMed: 11351018]
2. Popovic, DB. Neural Prostheses for Movement Restoration. In: Moore, J.; Zouridakis, G., editors. Biomedical Technology and Devices Handbook. CRC Press LLC; 2004. p. 28-1.
3. Mushahwar VK, Jacobs PL, Normann RA, Triolo RJ, Kleitman N. New functional electrical stimulation approaches to standing and walking. J Neural Eng 2007;4:S181–97. [PubMed: 17873417]
4. Lau B, Guevremont L, Mushahwar VK. Strategies for generating prolonged functional standing using intramuscular stimulation or intraspinal microstimulation. IEEE Trans Neural Syst Rehabil Eng 2007;15:273–85. [PubMed: 17601198]
5. Saigal R, Renzi C, Mushahwar VK. Intraspinal microstimulation generates functional movements after spinal-cord injury. IEEE Trans Neural Syst Rehabil Eng 2004;12:430–40. [PubMed: 15614999]
6. Bamford JA, Putman CT, Mushahwar VK. Intraspinal microstimulation preferentially recruits fatigue-resistant muscle fibres and generates gradual force in rat. J Physiol 2005;569:873–84. [PubMed: 16239281]
7. Gaunt RA, Prochazka A, Mushahwar VK, Guevremont L, Ellaway PH. Intraspinal Microstimulation Excites Multisegmental Sensory Afferents at Lower Stimulus Levels Than Local α-Motoneuron Responses. J Neurophysiol 2006;96:2995–3005. [PubMed: 16943320]
8. Biran R, Martin DC, Tresco PA. Neuronal cell loss accompanies the brain tissue response to chronically implanted silicon microelectrode arrays. Exp Neurol 2005;195:115–26. [PubMed: 16045910]
9. Agnew WF, McCreery DB. Considerations for safety with chronically implanted nerve electrodes. Epilepsia 1990;31:S27–32. [PubMed: 2226363]
10. Mortimer, JP. Motor Prostheses. In: Brooks, VD., editor. Motor Control. Vol. II. Bethesda, MA: American Physiological Society; 1981. p. 155-87.
11. McCreery DB, Agnew WF, Yuen TG, Bullara L. Charge density and charge per phase as cofactors in neural injury induced by electrical stimulation. 1990;37:996–1001.
12. McCreery D, Pikov V, Lossinsky A, Bullara L, Agnew W. Arrays for chronic functional microstimulation of the lumbosacral spinal cord. IEEE Trans Neural Syst Rehabil Eng 2004;12:195–207. [PubMed: 15218934]
13. Yakovenko S, Kowalczewski J, Prochazka A. Intraspinal stimulation caudal to spinal cord transections in rats. Testing the propriospinal hypothesis. J Neurophysiol 2007;97:2570–4. [PubMed: 17215510]
14. Guevremont L, Renzi CG, Norton JA, Kowalczewski J, Saigal R, Mushahwar VK. Locomotor-related networks in the lumbosacral enlargement of the adult spinal cat: activation through intraspinal microstimulation. IEEE Trans Neural Syst Rehabil Eng 2006;14:266–72. [PubMed: 17009485]
15. Nicolopoulos-Stournaras S, Iles JF. Motor neuron columns in the lumbar spinal cord of the rat. J Comp Neurol 1983;217:75–85. [PubMed: 6875053]

16. Shi SR, Liu C, Taylor CR. Standardization of immunohistochemistry for formalin-fixed, paraffin-embedded tissue sections based on the antigen-retrieval technique: from experiments to hypothesis. J Histochem Cytochem 2007;55:105–9. [PubMed: 16982846]

17. Sedgewick, J. Scientific imaging with Photoshop: methods, measurement, and output. Berkeley, CA: New Riders; 2008. p. ixp. 301

18. Kikuchi H, Doh-ura K, Kawashima T, Kira J, Iwaki T. Immunohistochemical analysis of spinal cord lesions in amyotrophic lateral sclerosis using microtubule-associated protein 2 (MAP2) antibodies. Acta Neuropathol 1999;97:13–21. [PubMed: 9930890]

19. Gonzalez SL, Lopez-Costa JJ, Labombarda F, Deniselle MC, Guennoun R, Schumacher M, et al. Progesterone Effects on Neuronal Ultrastructure and Expression of Microtubule-associated Protein 2 (MAP2) in Rats with Acute Spinal Cord Injury. Cell Mol Neurobiol. 2008

20. Nacimiento W, Sappok T, Brook GA, Toth L, Schoen SW, Noth J, et al. Structural changes of anterior horn neurons and their synaptic input caudal to a low thoracic spinal cord hemisection in the adult rat: a light and electron microscopic study. Acta Neuropathol 1995;90:552–64. [PubMed: 8615075]

21. Grill WM, Norman SE, Bellamkonda RV. Implanted Neural Interfaces: Biochallenges and Engineered Solutions. Annu Rev Biomed Eng. 2009

22. Cope TC, Pinter MJ. The Size Principle: Still Working After All These Years. News in Physiological Sciences News Physiol Sci 1995;10:280–6.

23. Durkovic RG. Functional consequences of motor unit recruitment order reversals following spinal cord transection in cat. Somatosens Mot Res 2006;23:25–35. [PubMed: 16846957]

24. Heckman CJ. Alterations in synaptic input to motoneurons during partial spinal cord injury. Med Sci Sports Exerc 1994;26:1480–90. [PubMed: 7869883]

25. Frigon A, Rossignol S. Functional plasticity following spinal cord lesions. Prog Brain Res 2006;157:231–60. [PubMed: 17167915]

26. Munson JB, Foehring RC, Lofton SA, Zengel JE, Sypert GW. Plasticity of medial gastrocnemius motor units following cordotomy in the cat. J Neurophysiol 1986;55:619–34. [PubMed: 3701396]

27. Norenberg MD, Smith J, Marcillo A. The pathology of human spinal cord injury: defining the problems. J Neurotrauma 2004;21:429–40. [PubMed: 15115592]

28. Kwon BK, Tetzlaff W, Grauer JN, Beiner J, Vaccaro AR. Pathophysiology and pharmacologic treatment of acute spinal cord injury. Spine J 2004;4:451–64. [PubMed: 15246307]

29. Biran R, Martin DC, Tresco PA. The brain tissue response to implanted silicon microelectrode arrays is increased when the device is tethered to the skull. J Biomed Mater Res A 2007;82:169–78. [PubMed: 17266019]

30. Haberler C, Alesch F, Mazal PR, Pilz P, Jellinger K, Pinter MM, et al. No tissue damage by chronic deep brain stimulation in Parkinson's disease. Ann Neurol 2000;48:372–6. [PubMed: 10976644]

31. Mushahwar VK, Collins DF, Prochazka A. Spinal cord microstimulation generates functional limb movements in chronically implanted cats. Exp Neurol 2000;163:422–9. [PubMed: 10833317]

32. McConnell GC, Schneider TM, Owens DJ, Bellamkonda RV. Extraction force and cortical tissue reaction of silicon microelectrode arrays implanted in the rat brain. IEEE Trans Biomed Eng 2007;54:1097–107. [PubMed: 17554828]

33. Turner JN, Shain W, Szarowski DH, Andersen M, Martins S, Isaacson M, et al. Cerebral astrocyte response to micromachined silicon implants. Exp Neurol 1999;156:33–49. [PubMed: 10192775]

34. Yu WR, Westergren H, Farooque M, Holtz A, Olsson Y. Systemic hypothermia following spinal cord compression injury in the rat: an immunohistochemical study on MAP 2 with special reference to dendrite changes. Acta Neuropathol 2000;100:546–52. [PubMed: 11045677]

35. Gilerovich EG, Moshonkina TR, Fedorova EA, Shishko TT, Pavlova NV, Gerasimenko YP, et al. Morphofunctional characteristics of the lumbar enlargement of the spinal cord in rats. Neurosci Behav Physiol 2008;38:855–60. [PubMed: 18802763]

36. Edgerton VR, Tillakaratne NJ, Bigbee AJ, de Leon RD, Roy RR. Plasticity of the spinal neural circuitry after injury. Annu Rev Neurosci 2004;27:145–67. [PubMed: 15217329]

37. Polikov VS, Tresco PA, Reichert WM. Response of brain tissue to chronically implanted neural electrodes. J Neurosci Methods 2005;148:1–18. [PubMed: 16198003]

38. Rousche PJ, Normann RA. A method for pneumatically inserting an array of penetrating electrodes into cortical tissue. Ann Biomed Eng 1992;20:413–22. [PubMed: 1510293]

39. McCreery DB, Yuen TG, Bullara LA. Chronic microstimulation in the feline ventral cochlear nucleus: physiologic and histologic effects. Hear Res 2000;149:223–38. [PubMed: 11033261]

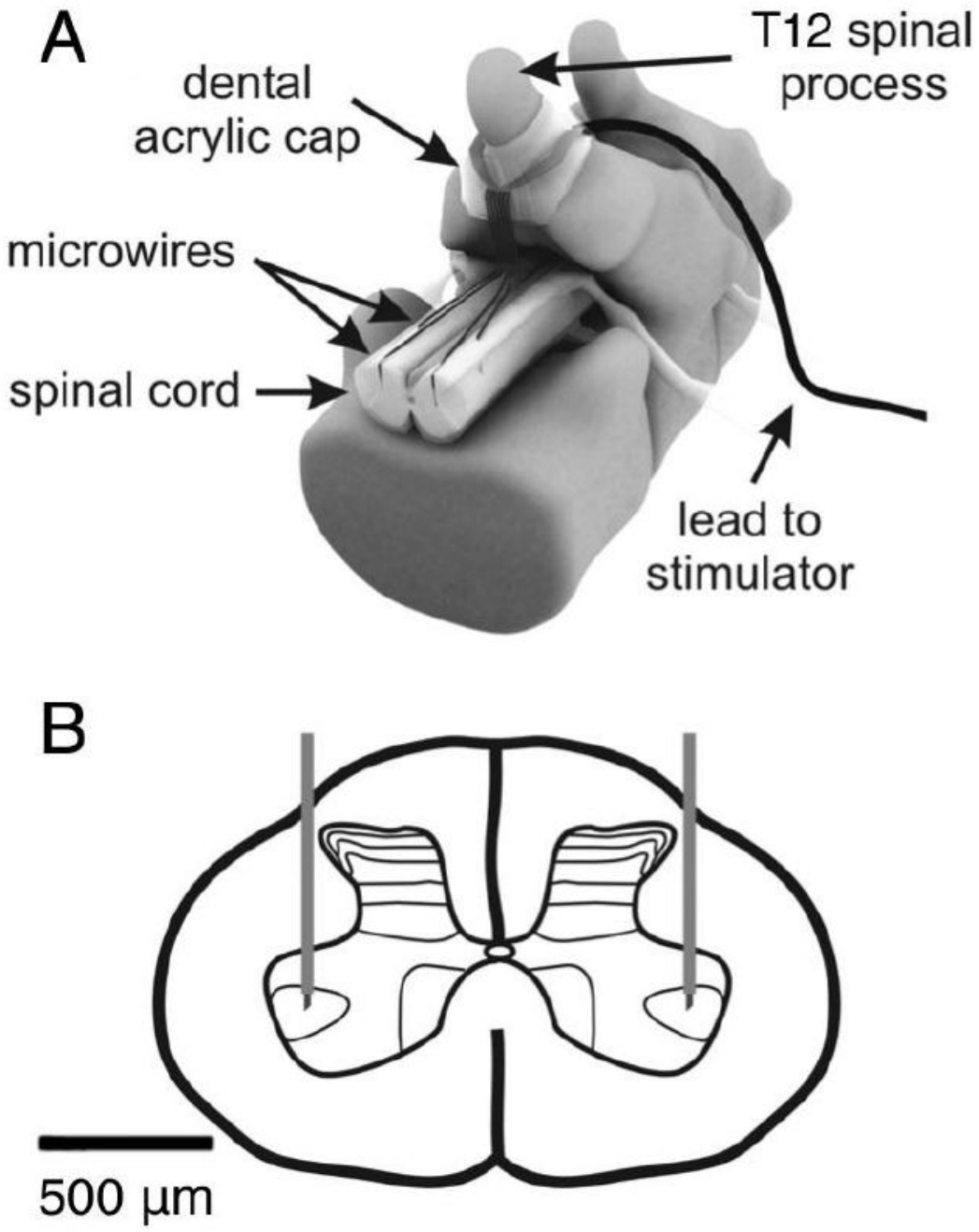

Figure 1. Schematic of the intraspinal implant

A laminectomy was performed at the T13 level in the rat to expose the lumbar enlargement for implantation of microwire arrays. (A) An example of an 8 microwire array is shown including the dental acrylic cap which secures the lead to the T12 spinous process. (B) Microwires with exposed tips are implanted bilaterally into the spinal cord with the tips targeting lamina IX in the ventral horn.

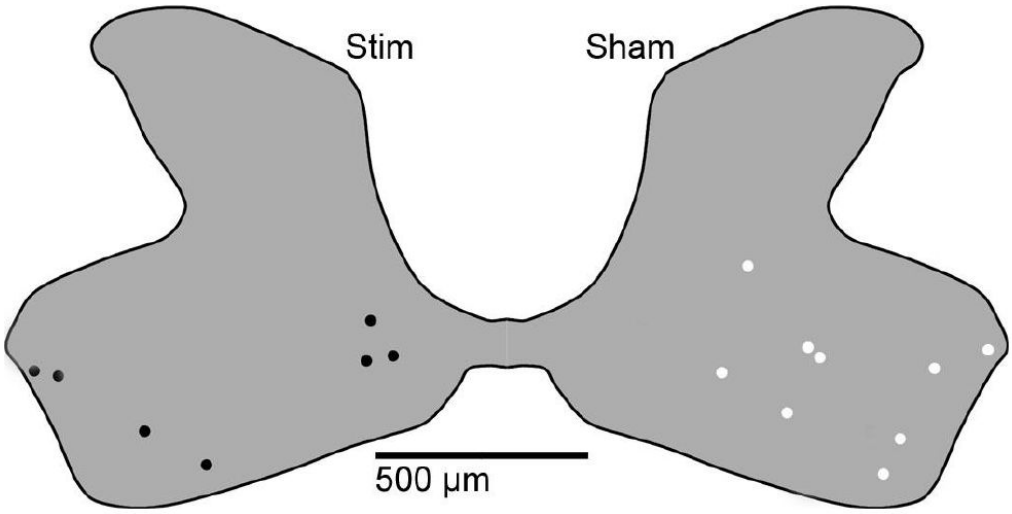

Figure 2. Summary of located microwire tips

The locations of stimulated and sham implanted microwire tips were identified in immunostained spinal cord tissue sections and a composite diagram was created to show their locations. We located 16 of 24 microwire tips, 9 from unpulsed microwires (shown in white) and 7 from pulsed microwires (shown in black). All tips were found within the grey matter of the ventral horn.

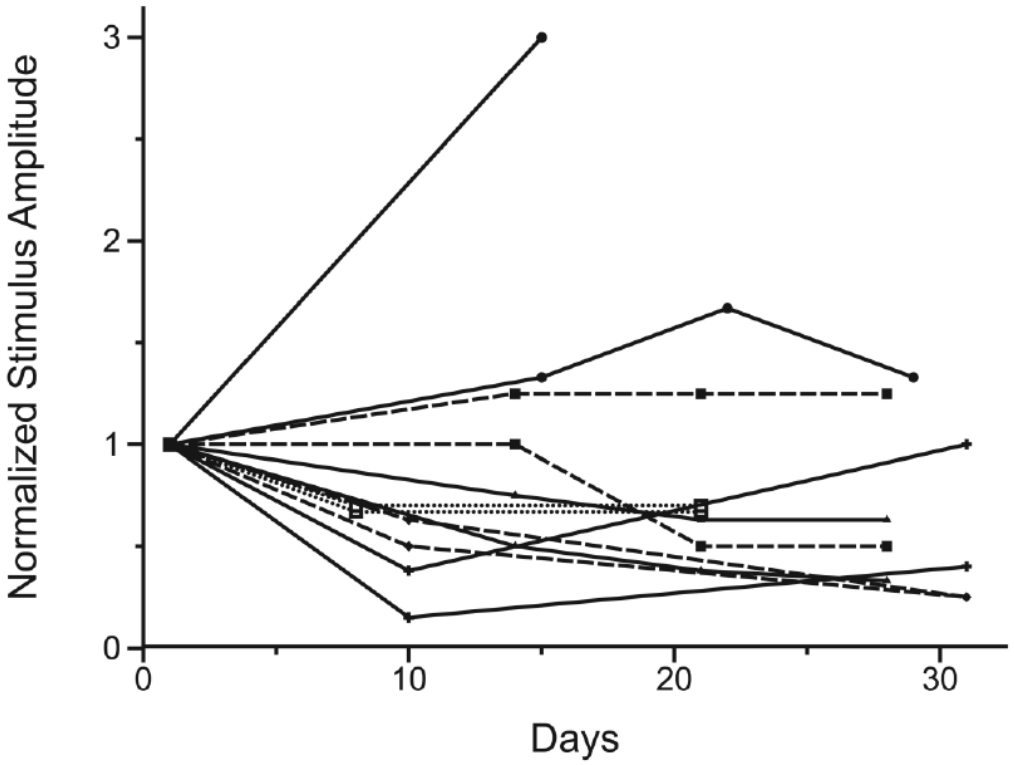

Figure 3. Activation thresholds from pulsed microwires during the 30 day stimulation period

ISMS thresholds for quadriceps muscle activation for the 12 stimulating microwires are shown normalized to their respective stimulus thresholds determined on the first day of stimulation. There was a significant decline in mean threshold amplitude from 118.2 μA ± 45.1 μA on the first day of stimulation to 67.8 μA ± 25.1 μA at the end of the stimulation period. The stimulus threshold for one microwire increased sharply before the microwire failed permanently on day 14. Of the remaining 11 microwires 8 had decreases in stimulus threshold, two had increases and one microwire had no overall change. Pairs of ipsilateral microwires in each animal are indicated by matching symbols and lines.

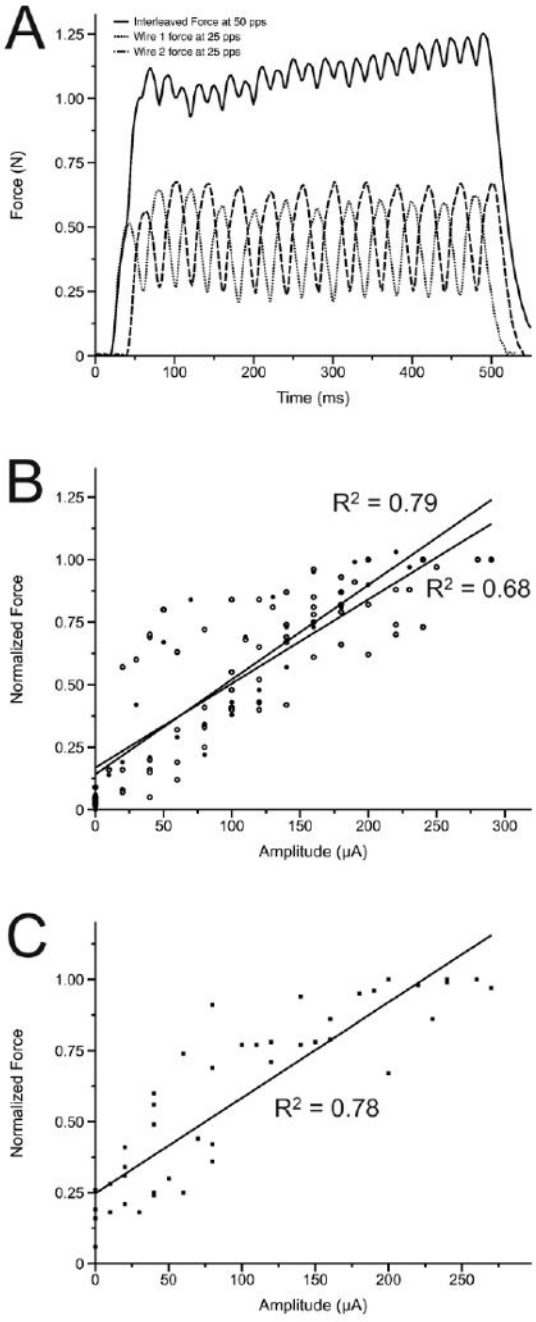

Figure 4. Force recruitment curves from intact and chronically spinalized and stimulated animals

(A) Examples are shown of forces recruited from individual ISMS microwires at 25 pps and from the resultant 50 pps product of interleaved stimulation through these microwires. (B) The relationship between normalized force and supra-threshold amplitude in intact animals from 6 individual microwires at 25 pps is shown in comparison to the same relationship generated by the resultant 50 pps product of interleaved stimulation in the same intact animals. (C) Following 30 days of chronic spinal transection and ISMS the relationship between normalized force and supra-threshold amplitude is shown.

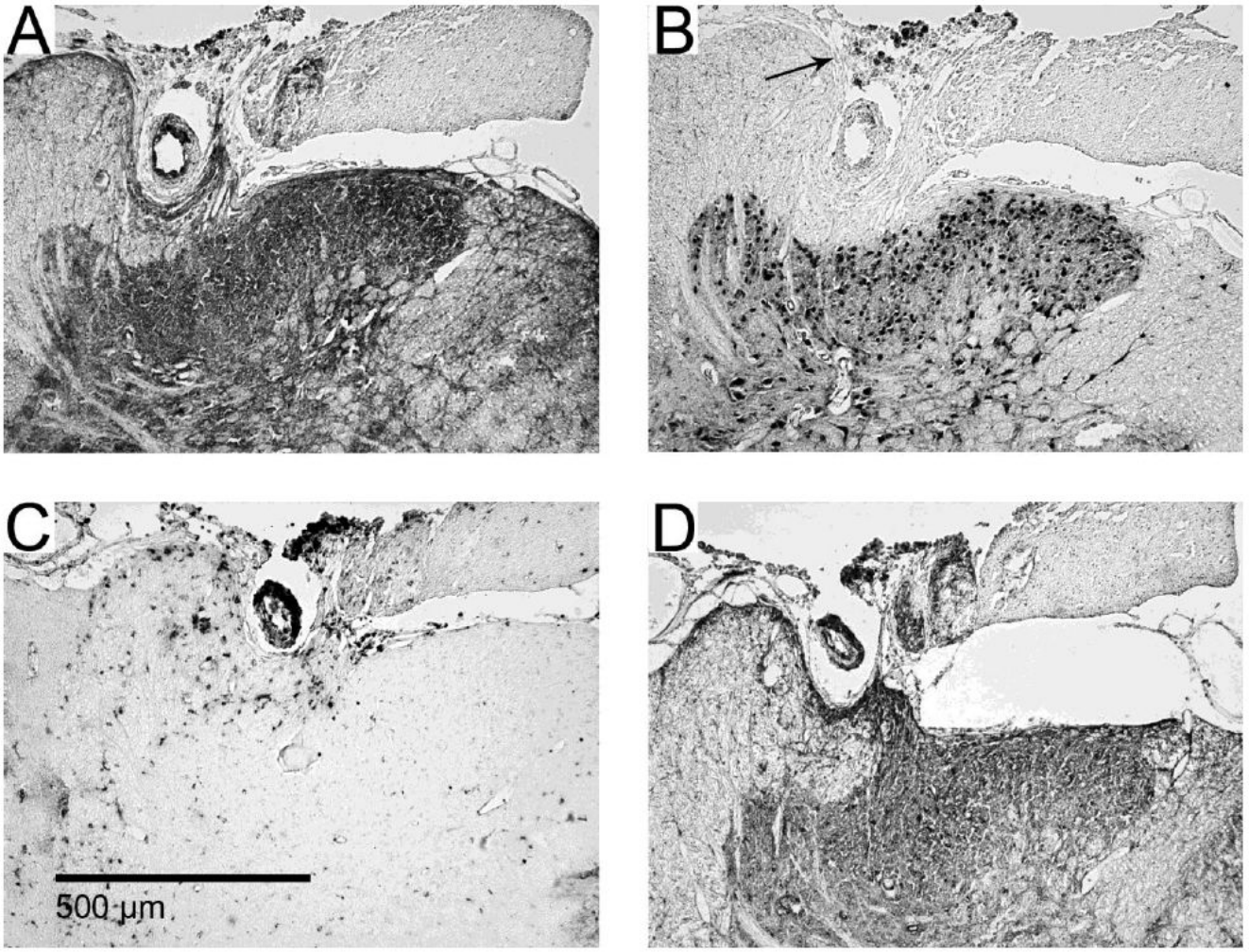

Figure 5. Dorsal horn invagination by implanted microwires

Serial images from one example (of two total) of dorsal horn damage due to invagination of microwires running across the dorsal surface of the spinal cord. Immunohistochemical stains for (A) Map-2, (B), NeuN, (C) ED-1 and (D) GFAP. Encapsulation of the microwire occurred with some deformation of the dorsal grey matter. Some pieces of insulation pulled off from the microwires and can be seen in panel B as dark spots indicated by the arrow.

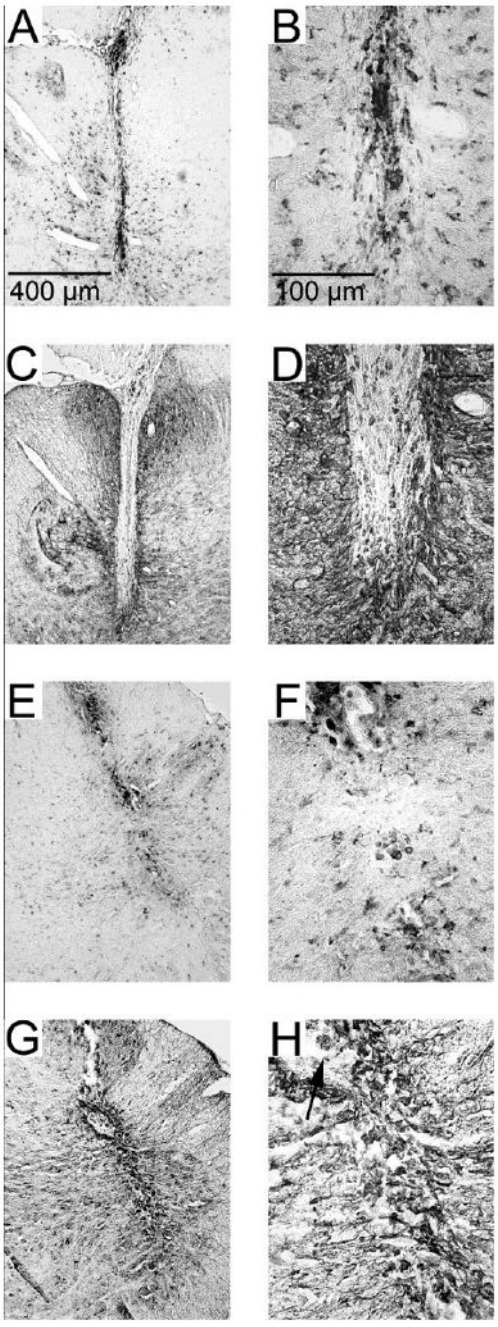

Figure 6. Pulsed and unpulsed microwire tracks

Examples of microwire tracks (A, C, E, G) and their tips (B, D, F, H). Unpulsed microwires (A, B, C, D) and pulsed microwires (E, F, G, H) displayed an ongoing inflammatory response as evidence by immunoreactivity for ED-1 (A, B, E, F). Encapsulation by a thin layer (< 50 μm) of GFAP immunoreactive astrocytes (C, D, G, H) was found along the entire track and at the microwire tip. The arrow in panel H indicates a piece of insulative material that was removed during explantation and was found in the microwire track.

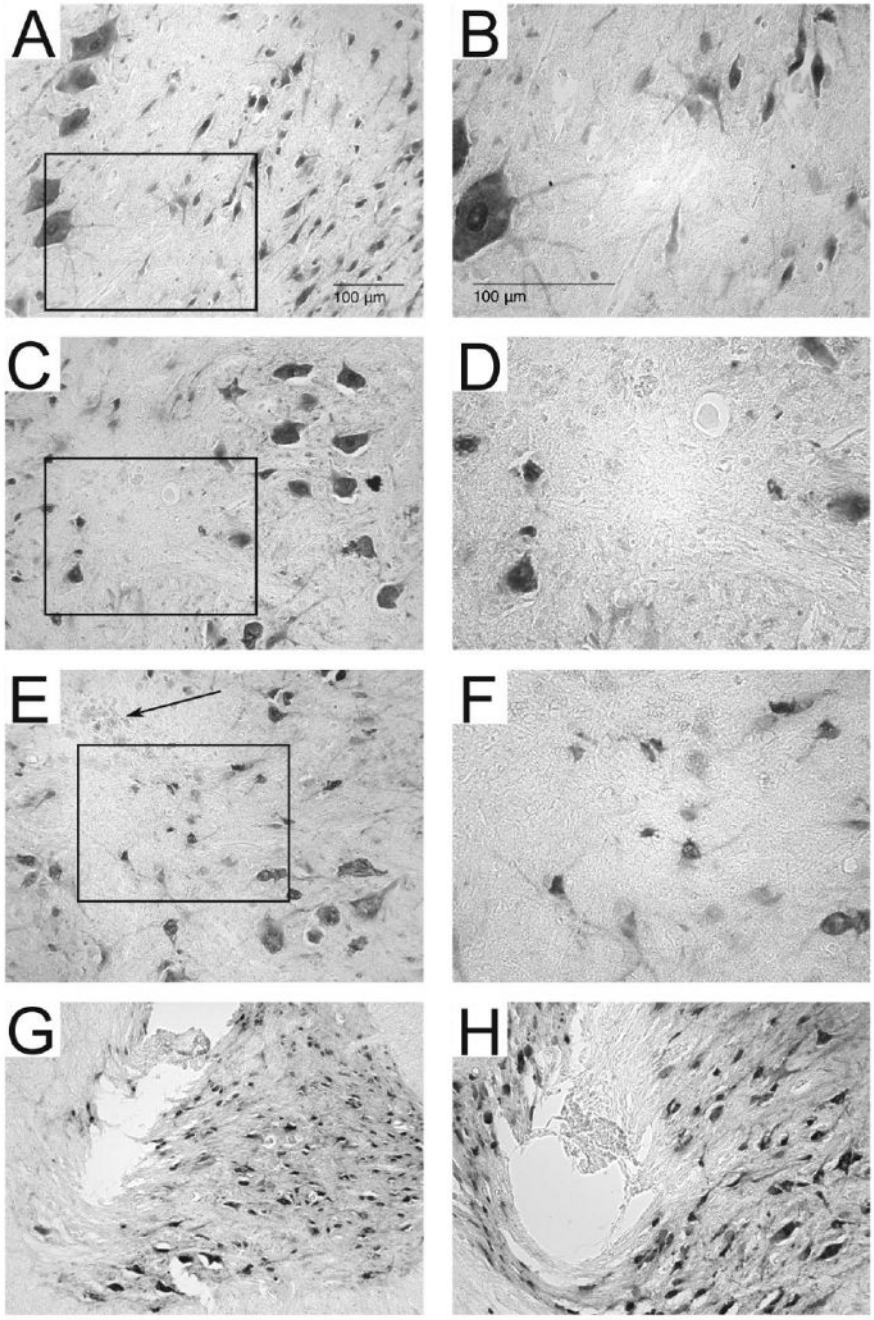

Figure 7. Neuronal density around microwires and in control tissue

Shown are representative sections immunoreacted with NeuN in spinal control tissue (A, B), around an unpulsed microwire track (C, D) and around a pulsed microwire track (E, F). Boxed outlines in A, C, E indicate the enlarged areas in B, D, F. Panels C and E are representative of the microwire track most commonly observed following explantation and illustrate the difficulty associated with locating microwire tracks on tissue sections stained for NeuN. Darkly stained $NeuN^+$ neurons can be seen surrounding the tracks of both pulsed and unpulsed microwire tracks. The microwire tracks themselves did not contain $NeuN^+$ cells and often displayed bits of the insulation which were stripped from the microwire tip during explantation (arrow in panel E). Explantation of the microwire tips caused tearing of the tissue surrounding

the microwire tracks in panels G and H. In panel G the tissue was pulled upwards along with the explanted microwire. In panel H the tissue subjacent to the microwire track can be seen to be compressed by the microwire, likely due to inadequate sharpening of the microwire tip.

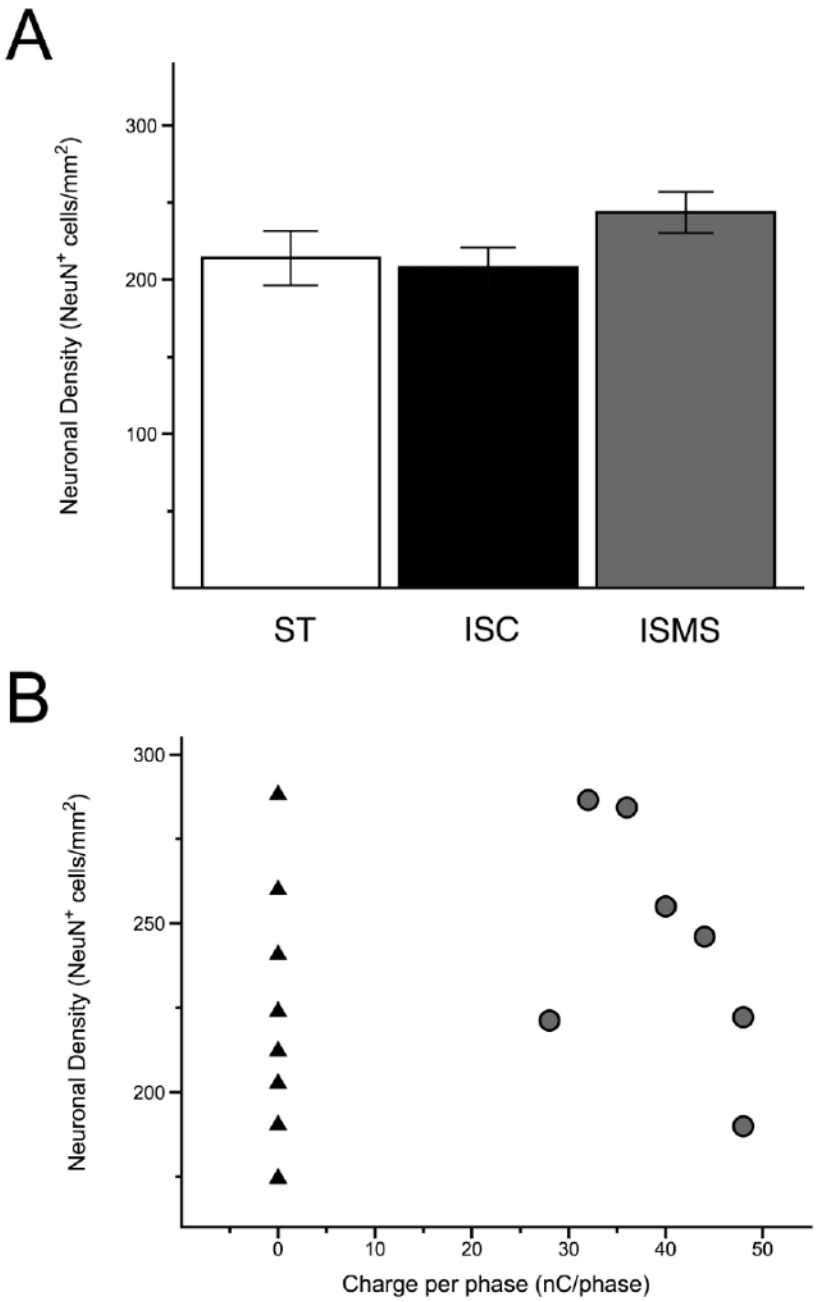

Figure 8. Quantification of neuronal density

Determination of neuronal density was made by counting NeuN immunoreactive cells in the ventral horn of ST, ISC and ISMS spinal tissue. (A) Neuronal density was not decreased in ISC or ISMS groups as compared to the spinal transected control. (B) When plotted against charge per phase, the range of neuronal density was virtually identical between the ISC side (black triangles) and the unstimulated ISMS side (grey circles). There was no significant correlation between increasing charge per phase and a decrease in neuronal density on the ISMS side.

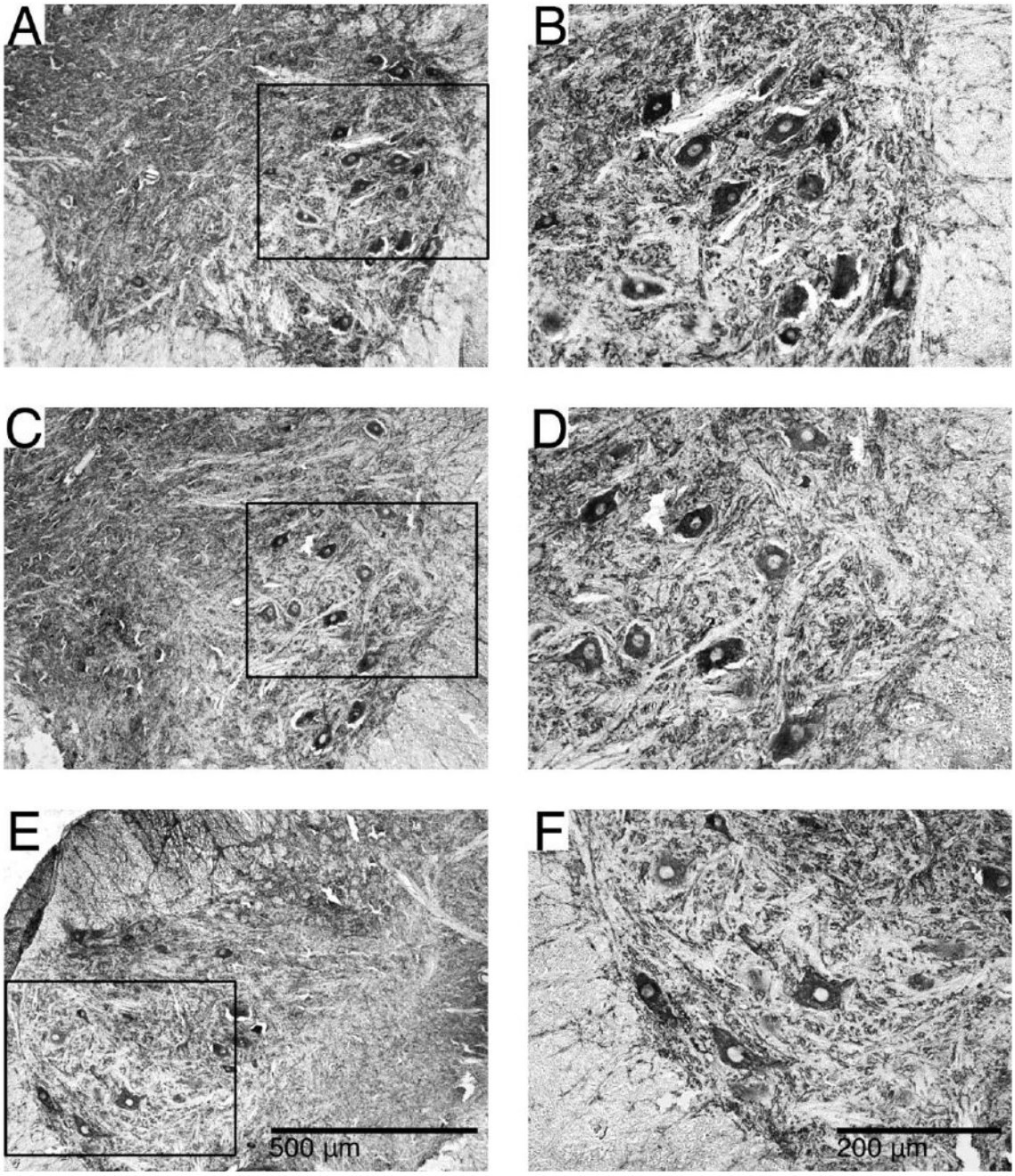

Figure 9. Cytoskeletal structure visualized with Map-2 immunoreactivity

Examples showing Map-2 immunoreactivity in the ventral horns of ST (A, B), ISMS (C, D) and ISC (E, F) groups. Black outlines in A, E, C indicate the enlarged areas in B, D, F. Strong staining of motoneurons and neurites in the ventral horn was seen including projections into the surrounding white matter. No apparent differences were noted between any of the groups.

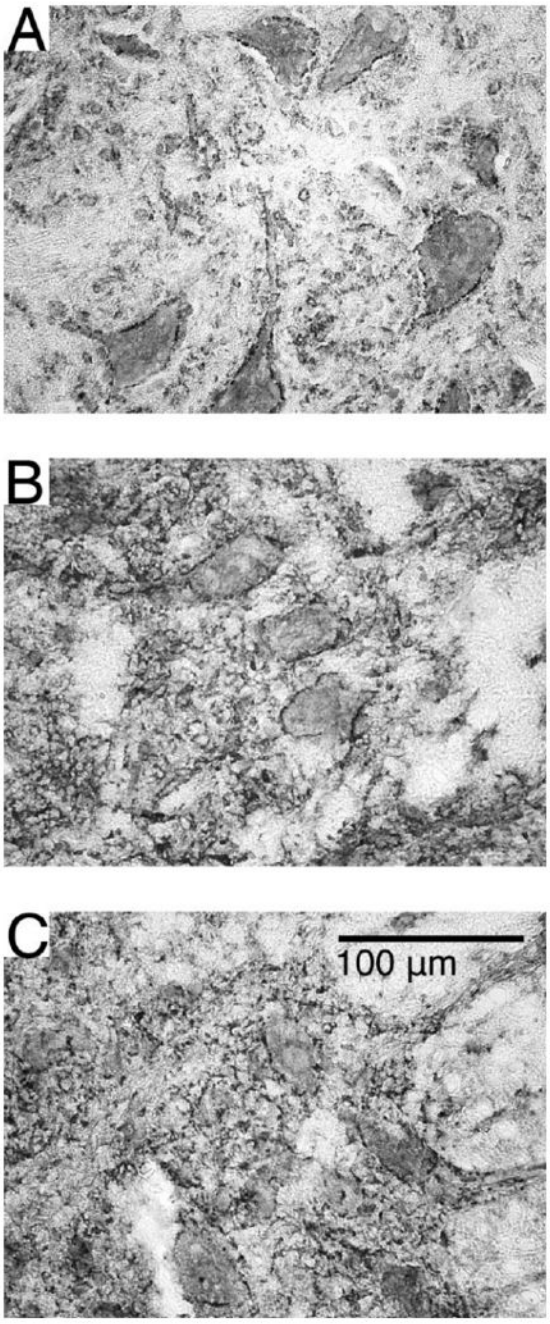

Figure 10. Synaptic inputs to motoneurons visualized with synaptophysin immunoreactivity

Representative sections displaying synaptophysin immunoreactivity in the ventral horns of ST (A), ISMS (B) and ISC (C) groups. Punctate and discontinuous staining around motoneurons in the ventral horn was seen suggesting axosomatic inputs at these locations. No apparent differences were noted between any of the groups.